

Modification strategy of thin film nanocomposite (TFN) forward osmosis membrane by introducing CNTs-ODA

Mostafa Narimani^a, Mehdi Ardjmand^{b,*}, Seyed Mostafa Tabatabaee Ghomsheh^c,
Ali Akbar Safekordi^a

^aDepartment of Chemical Engineering, Science and Research Branch, Islamic Azad University, Tehran, Iran,
emails: mostafa_narimani2005@yahoo.com (M. Narimani), safekordi@sharif.edu (A.A. Safekordi)

^bDepartment of Chemical Engineering, South Tehran Branch, Islamic Azad University, Tehran, Iran,
email: m_arjmand@azad.ac.ir (M. Ardjmand)

^cDepartment of Chemical Engineering, Mahshahr Branch, Islamic Azad University, Mahshahr, Iran,
email: m.mahshahruni@gmail.com (S.M.T. Ghomsheh)

Received 3 July 2019; Accepted 16 March 2020

ABSTRACT

The purpose of this study was to characterize the novel thin film nanocomposite (TFN) forward osmosis (FO) membrane. Generally in FO membrane construction, the water flux is mainly determined by the support layer, while the selectivity is by the active layer of the FO membrane. Therefore, both support and active layer designing are overemphasized by addressing new materials and modifications of them to overcome the main challenges of FO processes. In this regard poly(dioxanone), select as a material used in support layer fabrication and polyamide (PA) active layer modified with carbon nanotubes-octadecylamine (CNTs-ODA). The effect of CNTs-ODA concentration was investigated on the roughness, membrane morphology, chemical composition, and FO performance. It was found that the addition of modified CNTs in the manufacturing of the FO membrane undoubtedly enhances the water flux, reduces reverse salt flux, and minimizes the membrane fouling. Also, this modification has more comprehensive potential to changes the selectivity of TFN FO membranes.

Keywords: Forward osmosis; Modification; Thin film nanocomposite; Carbon nanotube

1. Introduction

Forward osmosis as a full-fledged water desalination process, has received increased attract in both experimental research and industrial development recently [1]. The osmotic pressure differential between two solutions of different concentrations (feed solution and draw solution) acts as the driving force to transport the water from a semi-permeable FO membrane [2,3]. So, there is no need to apply external energy which results in a low fouling tendency of the FO membrane. Other advantages of this method are high selectivity, lower fouling propensity, and higher water recovery [4–6]. However, all drawbacks of the FO process

such as membrane fouling originated from internal concentration polarization (ICP), lower flux, and reverse salt diffusion limit the performance of the FO applications. Therefore, the number of studies related to improving FO membranes that solve these problems are increasing in the applications [7].

To achieve a desirable FO separation performance, an FO membrane should have great qualities such as high water flux, high salt rejection, good stability, and favorable anti-fouling property [8]. In the past few years, various membranes have been investigated for FO applications. Currently, used FO membranes are mostly asymmetric thin film nanocomposite (TFN) membranes that prepared by

* Corresponding author.

interfacial polymerization. However, ICP is one of a major problem when asymmetric TFN membrane was used for the FO process. Therefore, efforts have focused on increasing the properties of TFN by designing both support and active layer by new materials [9,10], manufacturing methods [11] to overcome the main challenges of FO processes.

Since active layer with high roughness and large leaf-like structures are more prone to foulant accumulation and exhibit a dramatic decline in flux through the FO membranes, making it more difficult to improve the flux by a physical cleaning of them. For this reason, some of the research related to FO membranes has focused on active layer fabrication and modification. Recently, the utility of nanomaterials as additives for active layer modification to enhance membrane performance has been established [12].

According to the literature, researchers have begun to use graphene oxide (GO) [13], carbon nanotubes (CNTs) [14], zeolites [15,16], clay [17], mesoporous silica [18], and etc., into FO membrane modification. Among these additives, CNTs have become the focus of the research of polymer nanocomposite in the last few years due to the unique properties exhibited including good biocompatibility, high mechanical strength, chemical stability, flexibility, and good thermal stability [19,20]. One challenge in manufacturing TFN membranes containing CNTs is introducing increased CNTs with homogeneous distribution into the polymer matrix. Moreover low hydrophilicity of CNTs has become a major problem, which limits CNTs application in membrane modification. So, it is necessary to improve the dispersion and better compatibility of CNTs with polymer matrices, the CNTs must be modified by suitable agents. For improvement of hydrophilicity of CNTs lots of studies have been conducted. Amino and carboxylic CNTs have been employed to modify FO membranes and turned out that both have been effective [21,22].

Octadecylamine (ODA) as a functionalization agent with long-chain length can be prompt CNTs distribution in polymer matrices. On the other hand, the hydrophilic nature of ODA can significantly improve the FO membrane's performance.

In this work, in order to improve the hydrophilic and morphological properties of poly(dioxanone) PDO FO membrane, the CNTs that have been modified by ODA was added into the polyamide (PA) active layer of the FO membrane. The effect of the CNTs-ODA on the membrane surface morphology, chemical composition, and roughness of the novel TFN-FO membranes was systematically investigated using various characterization methods.

2. Experimental

2.1. Materials

PDO ($T_m = 110^\circ\text{C}$ and density = 1.38 g cm^{-3}) was purchased from Sigma-Aldrich Chemical Co., (Milwaukee, WI, USA) and used for fabricating the membrane substrate. PDO was dried in a vacuum oven at 60°C for 6 h before use. CNTs (average diameter = 4–6 nm, length = 50 μm , specific surface area = $>200 \text{ m}^2 \text{ g}^{-1}$) and ODA (melting point, 55°C – 57°C) were purchased from Rosseter Holdings Co., Ltd., (Cyprus). Analytical grade and high purity 1,1,2,2-tetrachloroethane, dimethylformamide (DMF), anhydrous tetrahydrofuran

(THF), dichloromethane, thionyl chloride (SOCl_2), nitric acid (HNO_3 , 70%), and ethanol were supplied from SAMCHUN (Korea). *m*-Phenylenediamine (MPD, 98%), trimesoyl chloride (TMC, 98%), and *n*-hexane ($>99\%$) were purchased from Merck (Darmstadt, Germany) and all employed for interfacial polymerization (IP). Sodium chloride and magnesium chloride were purchased from QRec.

2.2. Functionalization of CNTs by ODA

At first 10 g of CNTs were added to 300 mL solution of nitric acid (6 M) and then heated to 80°C for 8 h. After that, the mixture was washed with distilled water until the wash water was pH neutral and then dried in air to obtain CNTs with carboxylic groups. In the following steps, 10 g of oxidized CNTs were added to a 200 mL of thionyl chloride under stirring at the presence of 5 mL of DMF (80°C , 24 h). Subsequently, carboxyl CNTs were centrifuged and the dark supernatant was separated and the remaining solid was added to THF. This mixture was re-centrifuged and the yellow-colored solution was discarded. Then the remaining solid was dried at room temperature. In the next step, the surface of CNTs was functionalized with ODA. For this purpose, 5 g of CNTs-COCL which was obtained in the previous step was added to 20 g of ODA and the mixture was heated to 100°C under stirring for 3 d. After cooling to room temperature, the mixture was washed three times with ethanol under sonication for 10 min to remove unreacted ODA. The resulting black solid product was dissolved in dichloromethane, and after centrifugation, the remaining black-colored solid was taken to dryness under vacuum.

2.3. Synthesis of PDO support layer

Asymmetric sublayer of PDO was prepared using the phase inversion method induced by immersion precipitation. At first, PDO (16 wt.%) was dissolved into the 1,1,2,2-tetrachloroethane solution and was sonicated at 25°C for 48 h to obtain a transparent mixture. After degassing for 2 d, the casting solution was homogeneously poured onto a glass plate and spread with a membrane applicator to be as thin as 250 μm at room temperature. The nascent membrane was evaporated at $25^\circ\text{C} \pm 1^\circ\text{C}$ for 15 s and then immersed in the water coagulation bath maintained at $25^\circ\text{C} \pm 1^\circ\text{C}$. After complete coagulation, the membrane was transferred to a water bath for 6 h at room temperature.

2.4. TFN membrane preparation

The PA layer of TFN membranes was prepared through interfacial polymerization on the surface of PDO substrates using TMC and MPD as monomers. In this way, different concentrations of CNTs-ODA were dispersed in MPD solution (0.2, 0.4, 0.6, and 0.8 wt.%) and sonicated for 1 h. Following that for the preparation of PA layer the MPD – (CNTs-ODA) solution was poured onto the surface of PDO substrate for 5 min. Subsequently, 0.15 wt.% of TMC in hexane solution was poured on the top surface of the PDO membrane substrate. After a certain time (1 min), the excess TMC solution was poured off the surface and the membrane

was heated in a vacuum oven at 60°C for further polymerization. After the formation of the skin layer on the PDO supporting membrane, the membrane was kept in distilled water until that it was tested.

2.5. Measurements of CNTs-ODA

The functional groups of CNTs-ODA were investigated using Fourier transform infrared spectroscopy (FTIR, model ALPHA T, Germany) over the wave number range of 400–4,000 cm^{-1} at ambient temperature. Thermogravimetric analysis (LECO TGA801 thermogravimetric analyzer, USA) was performed to further confirm whether the ODA groups were grafted onto the CNTs under nitrogen flow at a heating rate of 10°C min^{-1} .

2.6. Measurements of TFN FO membrane

A field emission scanning electron microscopy (KYKY EM3200, Japan) was used to observe the morphology of the TFN FO membranes surface that were coated with gold before the examination.

Atomic force microscopy (AFM) was carried out to analyze the surface roughness of the membranes with an AFM device (DME model C-26, Switzerland) using the tapping mode. Small squares of the prepared membranes (approximately 1 cm^2) were cut and glued on the glass substrate. The membrane surfaces were imaged in a scan size of 10 $\mu\text{m} \times 10 \mu\text{m}$.

The specific functional groups that are present in the samples were determined using an FTIR spectroscopy (model ALPHA T, Germany) over the wide spectral range of 600–3,800 cm^{-1} .

2.7. Evaluation of FO performance

The prepared TFN FO membranes were characterized for water flux and rejection studies using a lab-scale cross-flow FO filtration set up with an effective filtration area of

20.2 cm^2 . In these experiments active layer of FO membranes facing feed solution directly. The draw solution and feed solution were circulated by two peristaltic pumps at a constant flow rate of 0.2 L min^{-1} in a loop at each side of FO cell channels.

Both feed and draw solutions were maintained at 25°C \pm 1°C during all FO tests. The feed solution concentration and the draw solution weight were monitored with samples collected each half an hour for at least three times. Also, the conductivity of feed solution was automatically recorded by a conductivity meter (Mettler Toledo S230 model, Switzerland).

The water permeation flux (J_w) ($\text{Lm}^{-2} \text{h}^{-1}$) was determined by measuring the weight change of the feed solution over a predetermined time as follows [18]:

$$J_w = \frac{\Delta V}{A \Delta t} \quad (1)$$

where ΔV is the volume of water permeating through the membrane (L) over a given period of time Δt (h), and A is the effective area of the FO membrane (m^2).

The reverse salt flux, J_s ($\text{g m}^{-2} \text{h}$) was calculated from the concentration and volume change of the feed solution using the following equation [18]:

$$J_s = \frac{\Delta C V}{A \Delta t} \quad (2)$$

where C (g L^{-1}) is the feed solution concentration and V (L) is the volume of feed solution over Δt , respectively.

3. Results and discussion

3.1. Measurements of CNTs-ODA

The typical TGA thermograms of CNTs and CNTs-ODA are shown in Fig. 1. As observed pure CNTs showed a steady insignificant weight loss between 29°C and 600°C.

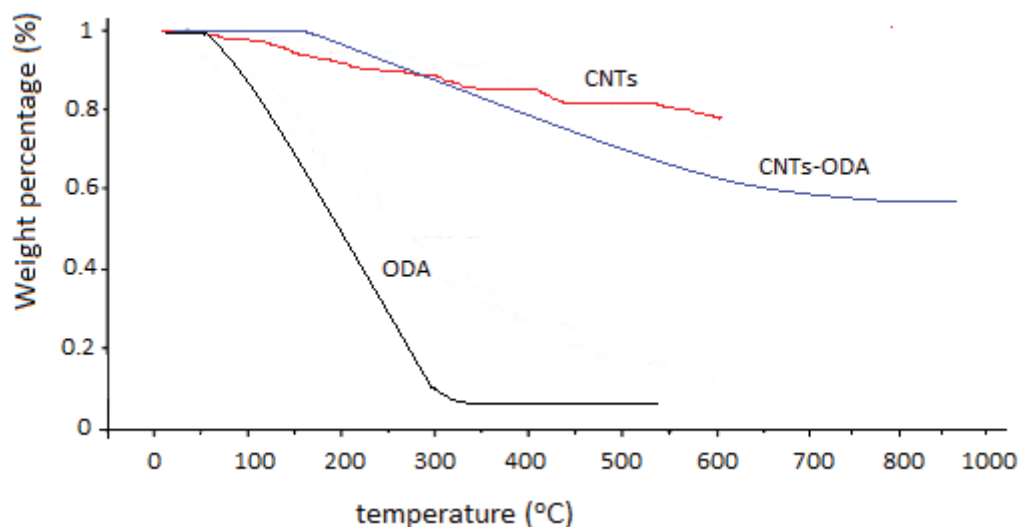


Fig. 1. TGA curves of CNTs, ODA, and CNTs-ODA.

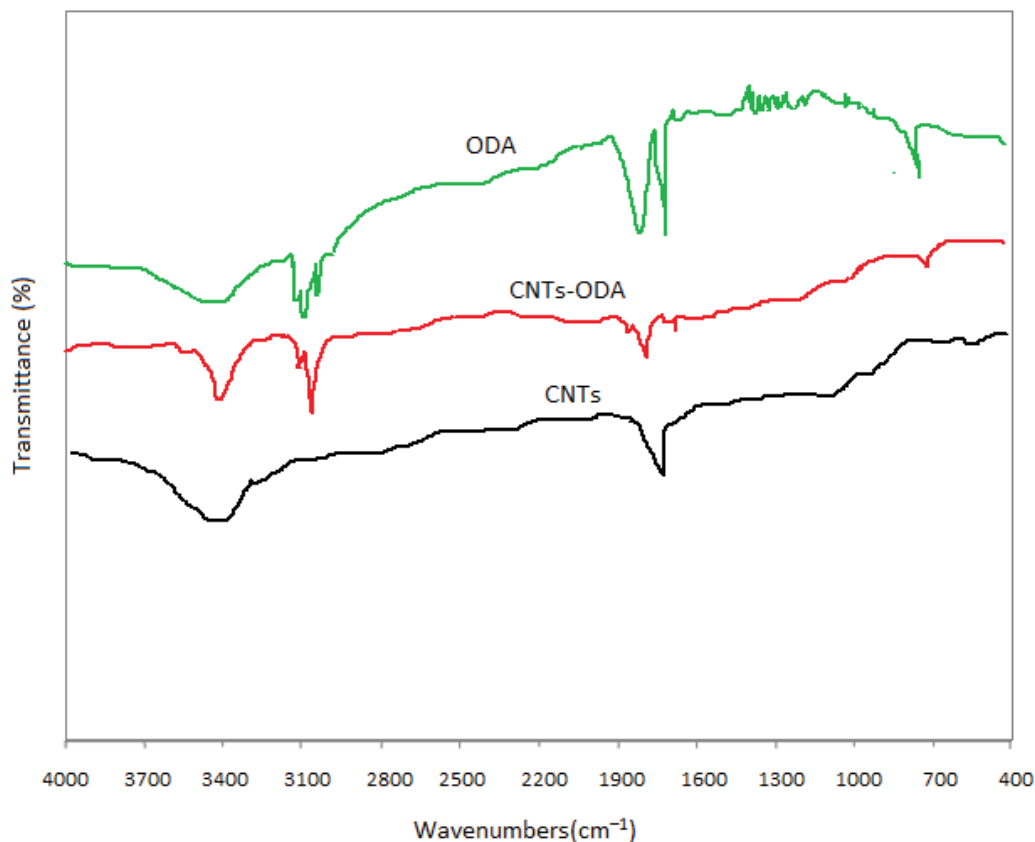


Fig. 2. FTIR spectra of CNTs, ODA, and CNTs-ODA.

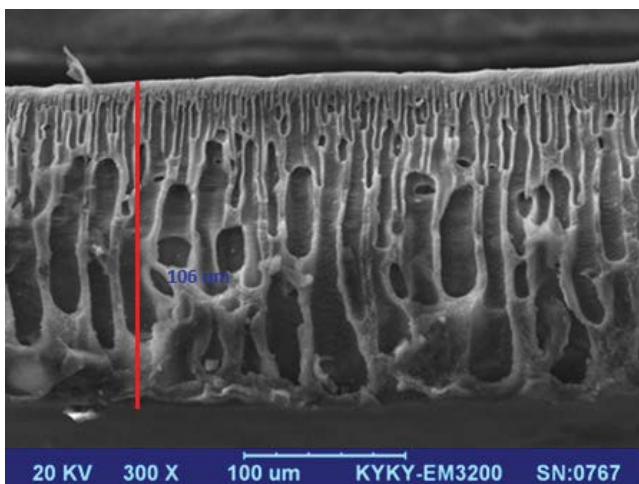


Fig. 3. SEM image of the support layer fabricated by PDO.

This weight loss for ODA was between its boiling point (55°C) and 310°C. The peak degradation temperature (T_{max}) of 205.7°C is exhibited for CNTs-ODA and its weight loss reached 40% at 800°C. This might be explained by the decomposition of the ODA chains.

Fig. 2 shows the FTIR spectrum of CNTs and modified CNTs. The CNTs represent characteristic O–H stretching vibration at 3,435 cm^{-1} . FTIR spectrum of ODA

is characterized by principal absorption peaks at 2,800–3,000 cm^{-1} (C–H, stretch, aliphatic). The characteristic bands for CNTs-ODA at 1,840 and 3,065 cm^{-1} assigned as the C–H stretching related to the ODA chains. Due to decreasing the number of OH groups by reaction with ODA in FTIR spectra of modified CNTs, the peak at 3,500 cm^{-1} became broader in comparison with pure CNTs.

3.2. Measurements of FO membrane

In TFN FO membrane fabrication, it is desirable that the support layers of the TFN FO membranes have high hydrophilicity, stability, and mechanical strength. These properties as well as low fouling tendencies increase the potential use of FO membranes [23,24]. For this purpose poly(dioxanone) is a good candidate due to its own special characteristics for support layer fabrication. Except for high mechanical and resistance properties of PDO, the unique ether bonds endow it with good flexibility [25]. Also, the finger-like structure of it as a support layer facilitates mass transport and reduces ICP in the FO process [26] (Fig. 3).

The PA layer on the top surfaces of FO membranes was observed as a typical ridge and valley appearance morphologically (Fig. 4). It is clear that the modified CNTs significantly affected on the surface structure of the TFN FO membranes. In the presence of CNTs-ODA, the molecular interaction between MPD and TMC decreases, so MPD molecules can't diffuse easily into organic phase.

So a smooth structure on the surface was obtained slightly. It's clear that an increase with a higher concentration of CNTs-ODA (up to 0.6 wt.%), significant agglomeration due to long-chain length of ODA takes place, so floccule appears on the membrane surface. The FTIR spectrum of the TFN FO membrane's active layer is presented in Fig. 5. The peaks around 1,500–1,700 cm^{-1} in the spectra could be attributed to the amide functional groups in active layer ($-\text{N}-\text{H}$ bending vibration, the aromatic ring breathing, and $-\text{C}=\text{O}$ stretching vibration, respectively). Also, the characteristic

absorptions were found at 2,961 cm^{-1} belonged to the C–H absorption of CH_2 groups of ODA. It was worth noting that there was a weak absorption near 3,500 cm^{-1} assigned to chain-end hydroxyl groups of CNTs. AFM images of the modified and unmodified active layer are shown in Fig. 6. These images confirm that the modified active layer has a smoother surface structure than the unmodified one. A low diffusion of the MPD into the solvent in the presence of ODA results in a slow reaction. Thus, the surface roughness of the impregnated active layer with ODA can

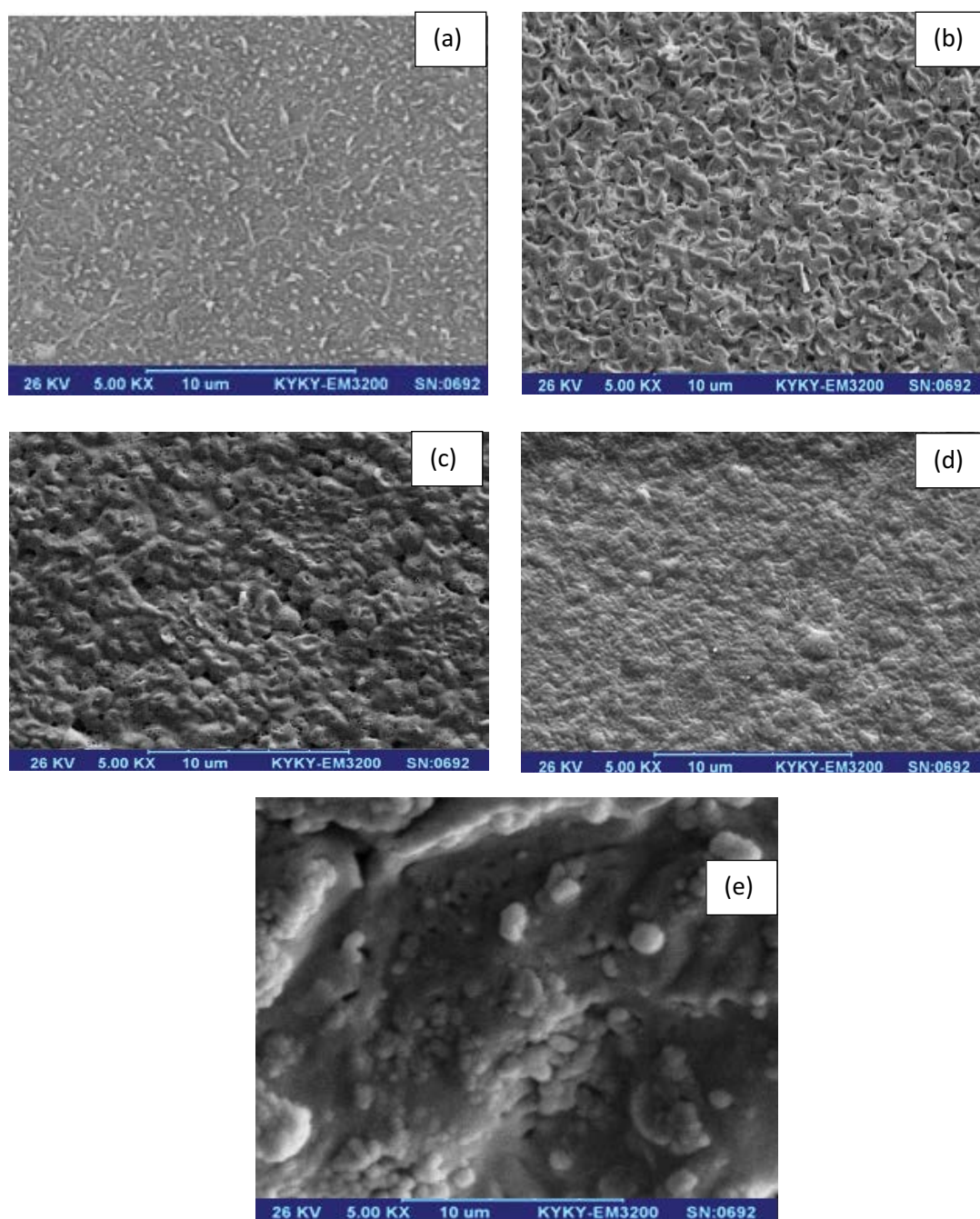


Fig. 4. SEM images of PA active layer of FO membranes modified with (a) 0 wt.% CNTs-ODA, (b) 0.2 wt.% CNTs-ODA, (c) 0.4 wt.% CNTs-ODA, (d) 0.6 wt.% CNTs-ODA, and (e) 0.8 wt.% CNTs-ODA.

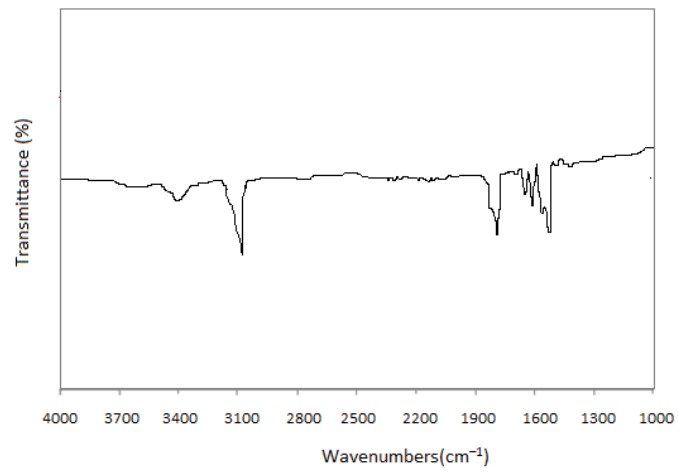


Fig. 5. FTIR spectra of the modified active layer of the TFN FO membrane.

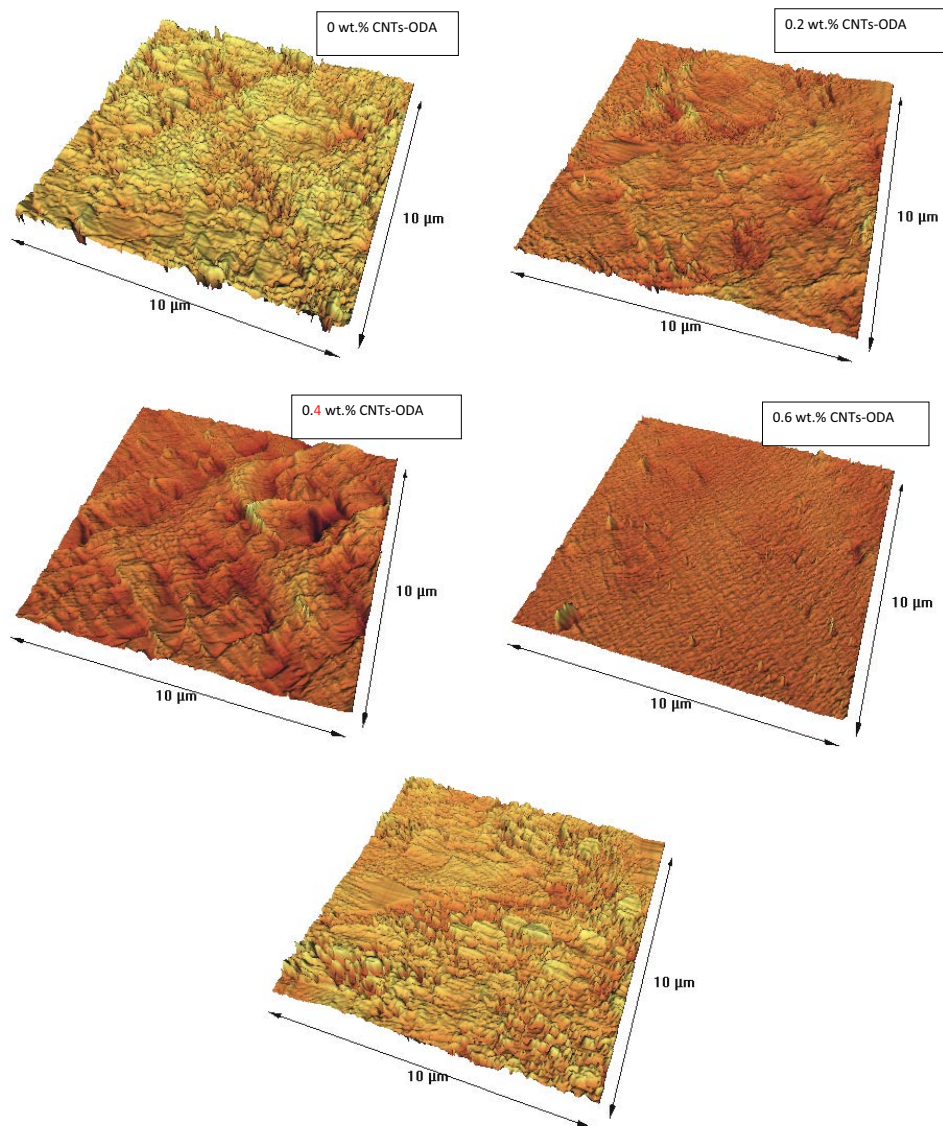


Fig. 6. AFM image of unmodified and modified TFN FO membranes.

be lower than the unmodified active layer. It's clear that an increase with a higher concentration of CNTs-ODA (up to 0.6 wt.%), significant agglomeration takes place, So the surface roughness increases consequently (Table 1). Also, the CNTs modification significantly achieved the homogeneous dispersion in the PA matrix that improved interfacial adhesion between CNTs and polymer matrix.

For measuring membranes' hydrophilicity, the contact angle analysis (HO-IAD-CAM-01 model) was conducted. Results show that the PDO substrate has a relatively hydrophilic nature ($\sim 63.2^\circ$). The contact angle of TFN membranes is also shown in Fig. 7. As shown in Fig. 4, the addition of modified CNTs in the PA layer greatly enhanced the membrane's hydrophilicity when the modified CNTs content is less than 0.4 wt.%. It can be explained in two aspects. First, modified CNTs made the membrane surface more hydrophilic due to the amines group of ODA. Besides, the addition of modified CNTs made membrane surface smoother and improve its hydrophilicity. The higher modified CNTs content ($>0.4\%$) will lead to a decrease in permeability because of pore blockage caused by excessive modified CNTs.

3.3. Evaluation of FO performance

For TFN FO performance evaluation, brackish water feed was used by dissolving NaCl in deionized water (1 M). $MgCl_2$ was considered as the draw solution in this study. Two parameters of water flux, reverse salt flux were used

Table 1
Roughness parameter of the active layer surface of FO membrane

Membrane	R_a (nm)
Unmodified PA layer	59.4
0.2 wt.% (CNT-ODA)	44.73
0.4 wt.% (CNT-ODA)	39.1
0.6 wt.% (CNT-ODA)	20.4
0.8 wt.% (CNT-ODA)	48.3

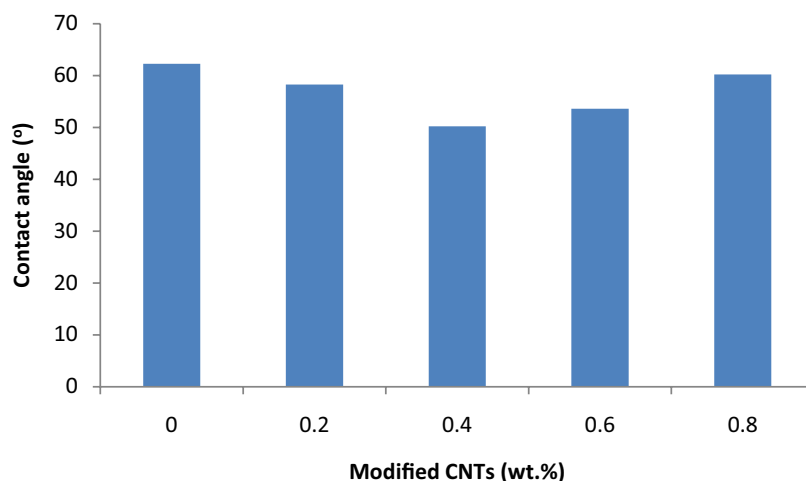


Fig. 7. Water contact angles of TFC and TFN membranes.

to assessing the functions of TFN FO membranes (Fig. 8). As can be observed in Fig. 8a, the permeation flux increases with the introduction of CNT-ODA (up to 0.6 wt.%), the permeate flux of all modified FO membranes follow by a low gradual decline with time. This behavior refers to low concentration polarization and fouling of the membranes due to applying the CNTs-ODA. The PA layer of CNT-ODA entrapped FO membrane was more hydrophilic than the unmodified one due to the higher affinity of ODA to water. On the other hand, the lower roughness of these membranes can be improved the hydrophilicity of them. Also, the resulting channels due to the CNTs-ODA usage in PA layer structure enhance the water permeability of FO membranes. As mentioned before, a further increase in the CNT-ODA concentration from 0.6 to 0.8 wt.%, results in CNTs-ODA coalesce and slightly decreases the water flux. These values of water flux in comparison with reported values in literature are promising [8,27,28].

The effect of draw solute concentration on the reverse salt flux is further studied, and the results are shown in Fig. 8b. As shown, the reverse salt flux increases with the increase in the draw solution concentration, which is attributed to their high osmotic pressure. Also, the modified FO membranes exhibited a lower reverse salt flux than the unmodified FO membrane. The reverse salt flux of modified FO membranes decreases with the increase of CNTs-ODA concentration (up to 0.4 wt.%) and then slightly increases. This trend is due to the reduction of the active layer's surface selectivity at high CNTs-ODA-concentrations.

By using CNTs-ODA as an additive to the PA active layer of the FO membrane, the resistance of the active layer to the solution was reduced, so the reverse salt flux was also relatively controlled.

4. Conclusion

Modification of novel FO membranes was carried out by the addition of different values of CNTs-ODA to the PA active layer. The PDO support layer and PA active layer of these FO membranes were synthesized using the phase inversion process and interfacial polymerization respectively. The effect

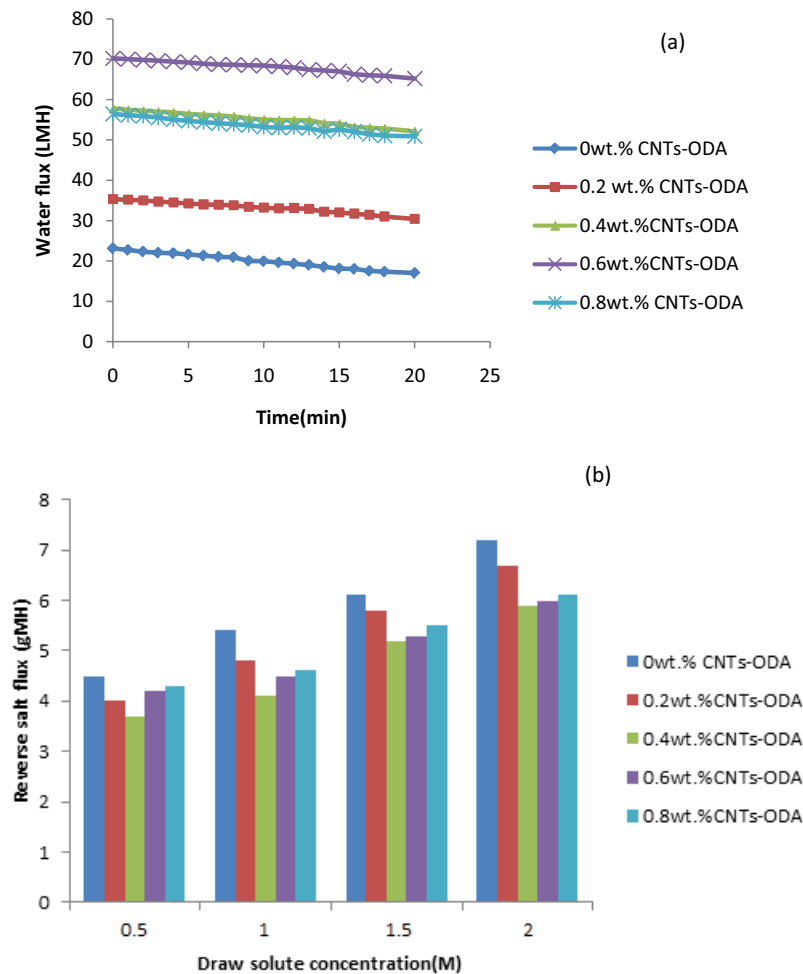


Fig. 8. Evaluation of prepared FO membrane performance (a) water flux and (b) reverse salt flux.

of the CNTs-ODA concentration was evaluated on the FO membrane specifications. Results show that PDO is a good candidate for the support layer of TFN FO membrane preparation due to its flexibility, strength, and high resistance. It is also recommended to investigate finger-like structure that facilitates mass transport and reduces ICP in the FO process. Furthermore, the addition of CNTs-ODA affects the hydrophilicity and roughness of the PA layer as well as enhances the FO performance of TFN FO membranes. It was revealed that the water flux of the CNTs-OD blended samples increases with increasing the CNTs-ODA content (up to 0.6 wt.%) (23.1–70.1 LMH) whereas their reverse salt flux showed an opposite tendency. With the further addition of CNTs-ODA (more than 0.4 wt.%), the reverse salt flux slightly increases. This trend was attributed to the reduction of active layer's surface selectivity at high CNTs-ODA concentrations. FO performance through the prepared membranes was noticeably affected by the CNTs-ODA addition.

References

- [1] S. Zhao, L. Zou, C.Y. Tang, D. Mulcahy, Recent developments in forward osmosis: opportunities and challenges, *J. Membr. Sci.*, 396 (2012) 1–21.
- [2] K. Lutchmiah, L. Lauber, K. Roest, D.J.H. Harmsen, J.W. Post, L.C. Rietveld, J.B. van Lier, E.R. Cornelissen, Zwitter ions as alternative draw solutions in forward osmosis for application in wastewater reclamation, *J. Membr. Sci.*, 460 (2014) 82–90.
- [3] Y. Liu, B. Mi, Combined fouling of forward osmosis membranes: synergistic foulant interaction and direct observation of fouling layer formation, *J. Membr. Sci.*, 407–408 (2012) 136–144.
- [4] Q. Liu, J. Li, Z. Zhou, J. Xie, J.Y. Lee, Hydrophilic mineral coating of membrane substrate for reducing internal concentration polarization (ICP) in forward osmosis, *Sci. Rep.*, 6 (2016) 19593–19602.
- [5] A. Shakeri, H. Salehi, F. Ghorbani, M. Amini, H. Naslhajian, Polyoxometalate based thin film nanocomposite forward osmosis membrane: superhydrophilic, anti-fouling, and high water permeable, *J. Colloid Interface Sci.*, 536 (2019) 328–338.
- [6] N. Ghaemi, Z. Khodakarami, Nano-biopolymer effect on forward osmosis performance of cellulosic membrane: high water flux and low reverse salt, *Carbohydr. Polym.*, 204 (2018) 78–88.
- [7] R.W. Baker, *Membrane Technology and Applications*, 2nd ed., John Wiley & Sons Ltd., UK, 2004, p. 538.
- [8] Y. Li, Y. Zhao, E. Tian, Y. Ren, Preparation and characterization of novel forward osmosis membrane incorporated with sulfonated carbon nanotubes, *RSC Adv.*, 8 (2018) 41032–41039.
- [9] M. Tian, Y.N. Wang, R. Wang, A.G. Fane, Synthesis and characterization of thin film nanocomposite forward osmosis membranes supported by silica nanoparticle incorporated nanofibrous substrate, *Desalination*, 401 (2017) 142–150.

- [10] A. Shakeri, H. Mighani, N. Salari, H. Salehi, Surface modification of forward osmosis membrane using polyoxometalate based open frameworks for hydrophilicity and water flux improvement, *J. Water Process Eng.*, 29 (2019) 100762.
- [11] W. Suwaileh, D. Johnson, S. Khodabakhshi, N. Hilal, Superior cross-linking assisted layer by layer modification of forward osmosis membranes for brackish water desalination, *Desalination*, 463 (2019) 1–12.
- [12] L. Shen, Y. Wang, Efficient surface modification of thin-film composite membranes with self-catalyzed tris(2-aminoethyl) amine for forward osmosis separation, *Chem. Eng. Sci.*, 178 (2018) 82–92.
- [13] D. Qin, Z. Liu, D.D. Sun, X. Song, H. Bai, A new nanocomposite forward osmosis membrane custom-designed for treating shale gas wastewater, *Sci. Rep.*, 5 (2015) 1–14.
- [14] L. Dumée, J. Lee, K. Sears, B. Tardy, M. Duke, S. Gray, Fabrication of thin film composite poly(amide)-carbon-nanotube supported membranes for enhanced performance in osmotically driven desalination systems, *J. Membr. Sci.*, 427 (2013) 422–430.
- [15] N. Ma, J. Wei, S. Qi, Y. Zhao, Y. Gao, C.Y. Tang, Nanocomposite substrates for controlling internal concentration polarization in forward osmosis membranes, *J. Membr. Sci.*, 441 (2013) 54–62.
- [16] N. Ma, J. Wei, R. Liao, C.Y. Tang, Zeolite-polyamide thin film nanocomposite membranes: towards enhanced performance for forward osmosis, *J. Membr. Sci.*, 405–406 (2012) 149–157.
- [17] B.K. Nandi, R. Uppaluri, M.K. Purkait, Effects of dip coating parameters on the morphology and transport properties of cellulose acetate-ceramic composite membranes, *J. Membr. Sci.*, 330 (2009) 246–258.
- [18] A. Shakeri, R. Razavi, H. Salehi, M. Fallahi, T. Eghbalazar, Thin film nanocomposite forward osmosis membrane embedded with amine-functionalized ordered mesoporous silica, *Appl. Surf. Sci.*, 481 (2019) 811–818.
- [19] Y. Wang, R. Ou, Q. Ge, H. Wang, T. Xu, Preparation of polyethersulfone/carbon nanotube substrate for high-performance forward osmosis membrane, *Desalination*, 330 (2013) 70–78.
- [20] X. Yang, Q. Wang, X. Qu, W. Jiang, Bound and unbound humic acids perform different roles in the aggregation and deposition of multi-walled carbon nanotubes, *Sci. Total Environ.*, 586 (2017) 738–745.
- [21] A. Tiraferri, C.D. Vecitis, M. Elimelech, Covalent binding of single-walled carbon nanotubes to polyamide membranes for antimicrobial surface properties, *ACS Appl. Mater. Interfaces*, 3 (2011) 2869–2877.
- [22] M. Amini, M. Jahanshahi, A. Rahimpour, Synthesis of novel thin film nanocomposite (TFN) forward osmosis membranes using functionalized multi-walled carbon nanotubes, *J. Membr. Sci.*, 435 (2013) 233–241.
- [23] G. Han, T.S. Chung, M. Toriida, S. Tamai, Thin-film composite forward osmosis membranes with novel hydrophilic supports for desalination, *J. Membr. Sci.*, 423–424 (2012) 543–555.
- [24] M. Yasukawa, S. Mishima, M. Shibuya, D. Saeki, T. Takahashi, T. Miyoshi, H. Matsuyama, Preparation of a forward osmosis membrane using a highly porous polyketone microfiltration membrane as a novel support, *J. Membr. Sci.*, 487 (2015) 51–59.
- [25] M.A. Sabino, G. Ronca, A.J. Muller, Heterogeneous nucleation and self nucleation of poly(p-dioxanone), *J. Mater. Sci.*, 35 (2000) 5071–5084.
- [26] A. Tiraferri, N.Y. Yip, W.A. Phillip, J.D. Schiffman, M. Elimelech, Relating performance of thin-film composite forward osmosis membranes to support layer formation and structure, *J. Membr. Sci.*, 367 (2011) 340–352.
- [27] M. Son, V. Novotny, H. Choi, Thin-film nanocomposite membrane with vertically embedded carbon nanotube for forward osmosis, *Desal. Water Treat.*, 57 (2016) 1–10.
- [28] E.S. Kim, G. Hwang, M. Gamal El-Din, Y. Liu, Development of nanosilver and multi-walled carbon nanotubes thin-film nanocomposite membrane for enhanced water treatment, *J. Membr. Sci.*, 394–395 (2012) 37–48.